BMC Pulmonary Medicine

RESEARCH

Open Access

A nomogram for predicting lymphovascular invasion in lung adenocarcinoma: a retrospective study

Miaomaio Lin[1], Xiang Zhao[1], Haipeng Huang[2], Huashan Lin[3] and Kai Li[1*]

Abstract

Backgroud Lymphovascular invasion (LVI) was histological factor that was closely related to prognosis of lung adenocarcinoma (LAC).The primary aim was to investigate the value of a nomogram incorporating clinical and computed tomography (CT) factors to predict LVI in LAC, and validating the predictive efficacy of a clinical model for LVI in patients with lung adenocarcinoma with lesions ≤ 3 cm.

Methods A total of 450 patients with LAC were retrospectively enrolled. Clinical data and CT features were analyzed to identify independent predictors of LVI. A nomogram incorporating the independent predictors of LVI was built. The performance of the nomogram was evaluated by assessing its discriminative ability and clinical utility.We took 321 patients with tumours ≤ 3 cm in diameter to continue constructing the clinical prediction model, which was labelled subgroup clinical model.

Results Carcinoembryonic antigen (CEA) level, maximum tumor diameter, spiculation, and vacuole sign were independent predictors of LVI. The LVI prediction nomogram showed good discrimination in the training set [area under the curve (AUC), 0.800] and the test set (AUC, 0.790), the subgroup clinical model also owned the stable predictive efficacy for preoperative prediction of LVI in lung adenocarcinoma patients, and both training and test set AUC reached 0.740.

Conclusions The nomogram developed in this study could predict the risk of LVI in LAC patients, facilitate individualized risk-stratification, and help inform treatment decision-makin, and the subgroup clinical model also had good predictive performance for lung cancer patients with lesion ≤ 3 cm in diameter.

Keywords Lymphovascular invasion, Lung adenocarcinoma, Computed Tomography, Nomogram

Background

Lung cancer is a major global health problem [1] with the highest morbidity and mortality among all malignant tumors [2]. Lung cancer cells mainly originate from the bronchial mucosal epithelium. Lung cancer can be divided into two main types, non-small cell lung cancer (NSCLC) and small cell lung cancer (SCLC), of which NSCLC is the most common pathological type [3]. Complete surgical resection is currently the most commonly used treatment for lung cancer. However, the 5-year survival rate of these patients is still unsatisfactory due to postoperative tumor recurrence and

*Correspondence:
Kai Li
doctorlikai@126.com
[1] Department of Radiology, The First Affiliated Hospital of Guangxi Medical University, Nanning, China
[2] Department of Radiology, People's Hospital of Guangxi Zhuang Autonomous, Nanning, China
[3] Department of Pharmaceutical Diagnosis, GE Healthcare, Shanghai, China

metastasis. Even patients with stage I or II NSCLC have low 5-year survival rate (30%–60%), and at least 30% of patients with stage I NSCLC experience tumor recurrence after complete resection. Lymphovascular invasion (LVI), defined as the infiltration of tumor cells in arteries, veins, or lymphatic vessels, has been shown to be the first step in local recurrence and distant spread of tumors [4].

As a pathological indicator, LVI can only be confirmed by puncture or postoperative biopsy. Therefore, identification of non-invasive predictors of LVI is of much clinical importance and can facilitate preoperative risk-stratification of patients with lung adenocarcinoma (LAC). Some studies have demonstrated that the maximum diameter and imaging findings of spiculation are closely related to the occurrence of LVI in LAC [5]. However, most of the previous studies are based on small sample size, and the reliability of the findings needs to be further verified. Our study had an advantage over previous studies in terms of the number of patients.,aiming to provide a more reliable reference for preoperative prediction of LVI in LAC.

Patients

Methods

This study was conducted as a single-center retrospective study from January 2016 to October 2021, The study received approval from the Research Ethics Committee at (No. 2023-E153-01).All patients with a pathological diagnosis of LAC between January 2016 and October 2021 were screened from the medical records of the First Affiliated Hospital of Guangxi Medical University. Inclusion criteria: (1) Patients who underwent unenhanced chest CT scan within two weeks before surgery; (2) patients for whom LVI status (positive or negative) was confirmed after surgery; (3) availability of satisfactory CT images for analysis; (4) no history of any other type of lung tumor. Exclusion criteria: (1) Patients with incomplete clinical, imaging or pathological data; (2) patients who received chemotherapy or radiotherapy before surgery. Finally, a total of 450 patients with LAC [243 males and 207 females; mean age, 57.88 years (range, 23–81)] were included in this study. A schematic illustration of the study selection criteria is shown in Fig. 1.

The study population was randomly divided into a training set and a test set at a ratio of 7: 3. The training set of the nomogram included 171 LVI-positive patients and 145 LVI-negative patients, while the test set included 73

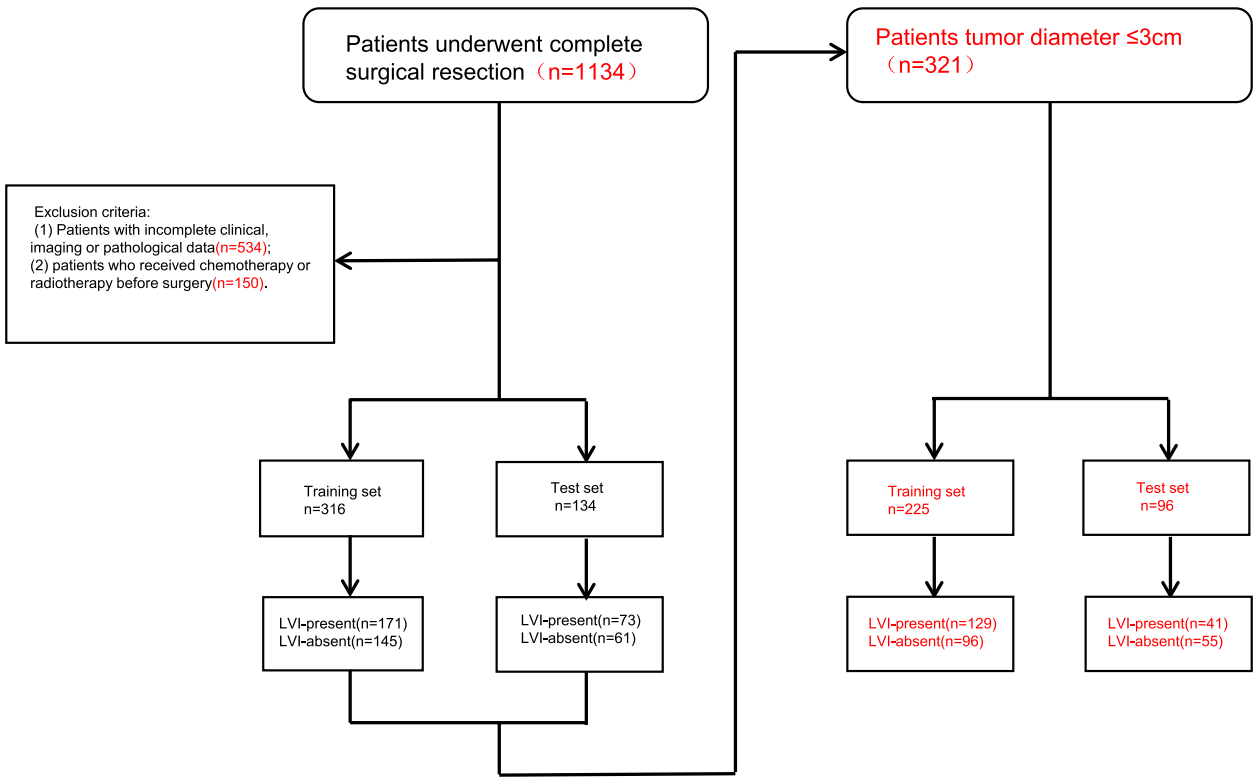

Fig. 1 Flowchart illustrating the inclusion and exclusion criteria for this study

LVI-positive patients and 61 LVI-negative patients, and the training set of the subgroup clinical model included 96 LVI-positive patients and 129 LVI-negative patients, while the test set included 41 LVI-positive patients and 55 LVI-negative patients.

CT imaging

All patients underwent unenhanced chest CT with a 256-row detector CT (Revolution CT, GE Healthcare, USA).. The CT scan parameters were as follows: tube voltage, 120 kVp; tube current (using automatic tube current modulation technique), 80–100 mA; pitch, 0.992:1; rotation time, 0.50 s; matrix, 512×512; reconstructed slice thickness, 1.25 mm;reconstructed algorithm,standard algorithm. All scans were performed with the patient in supine position with holding of breath. The scanning area covered the entire chest.

Clinical data and CT features analysis

Patient clinical data were collected through the hospital electronic medical record system. The clinical data were as follows: (1) age; (2) gender; (3) smoking history; (4) preoperative CEA level (>5 mg/ml was defined as positive). All images were evaluated independently by two radiologists (12 and 20 years of experience in chest imaging diagnosis, respectively) who were blinded to clinic-pathologic details. The final results were determined by consensus. The CT morphological features were defined based on previous studies on lung cancer [6, 7]. CT-reported tumor maximum diameter (the maximum cross-sectional diameter of the tumor); tumor location (left or right lung); border (sharp or ill-defined); shape (regular or irregular; "regular shape" was defined as round or ovoid); spiculation (present or absent; "spiculation" was defined based on the unenhanced CT lung window: short, radial, unbranched shadows extending from the edge of the tumor to the surrounding lung parenchyma and not connected to the pleura) (Fig. 2a); lobulation (present or absent; "lobulation" was defined as uneven lobulated contour of the tumor surface) (Fig. 2b); vacuole sign (present or absent; "vacuole sign" was defined as intratumoral round or ovoid air attenuation with a diameter < 5 mm) (Fig. 2c, d); air bronchogram (present or absent; "air bronchogram" was defined as presence of air-filled bronchi in the tumor) (Fig. 2e); pleural indentation (present or absent; "pleural indentation" was defined as a linear or tentorial shadow between the tumor and the pleura, or a star-shaped shadow) (Fig. 2f).

Pathological evaluation

All surgical specimens were processed for histopathological examination and the sections were stained with hematoxylin and eosin (H&E) stain (Fig. 3a), immunohistochemical stain for CD34 (a transmembrane glycoprotein expressed on the surface of normal vascular endothelial cells(Fig. 3b), a commonly used vascular endothelial cell marker) or D2-40 (a marker for lymphatic endothelial cells), if necessary (Fig. 3c). LVI was defined as microscopic demonstration of the presence of tumor

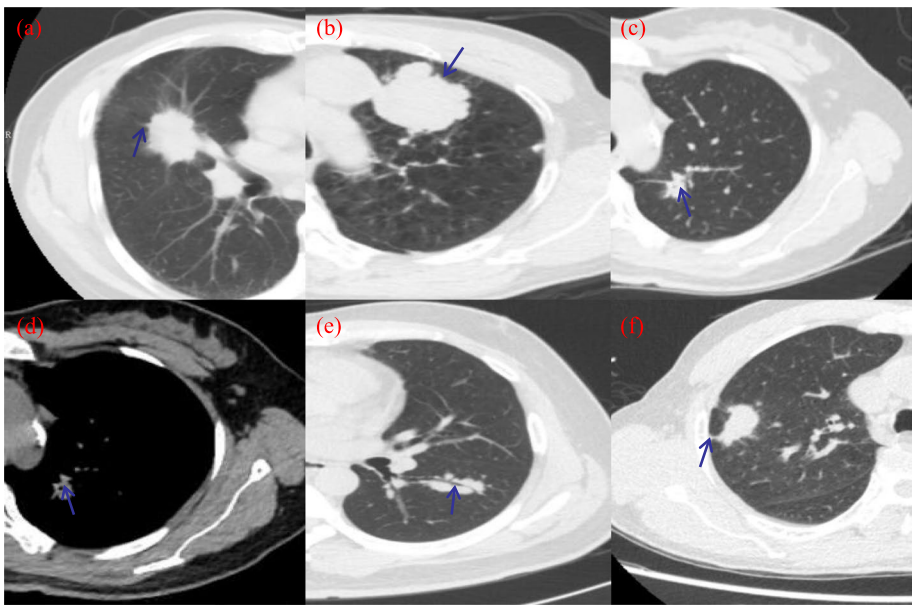

Fig. 2 Representative computed tomography images showed morphological features of lung adenocarcinoma. Spiculation (**a**), lobulation (**b**), vacuole sign (**c**, **d**), air bronchogram (**e**), and pleural indentation (**f**) (shown as arrows)

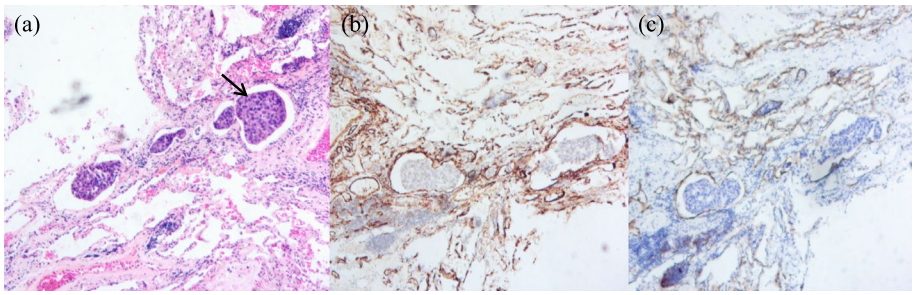

Fig. 3 Assessment of lymphovascular invasion in lung adenocarcinoma. Photomicrograph (H and E, × 100) showed detached clusters of tumor cells (arrow) inside the vascular lumen beyond the edge of the tumor, suggesting lymphovascular invasion (**a**). Immunohistochemical staining for CD34 (**b**) and D2-40 antibodies indicative of lymphovascular invasion in lung adenocarcinoma (**c**)

cells in the vessels [8]. Presence of either blood vessel invasion or lymphatic invasion was considered as LVI-positive [9]. Histopathological results were independently evaluated by two pathologists (5 and 10 years of experience, respectively), both of whom were blinded to the pathological records. In case of any disagreement between the final decision was made by another senior pathologist.

Clinical independent predictor selection and model construction

The patients were randomly divided into training and test set according to 7:3, and statistically significant variables were screened in the training set using univariate logistic regression analysis, and variables with $P < 0.05$ in the univariate logistic regression analysis were further included in the multivariate logistic regression analysis, so as to screen the clinical factors with independent predictive efficacy. Finally, a clinical prediction model was constructed using the logistic regression algorithm, and the predictive efficacy of the model was evaluated using the area under the curve (AUC), accuracy, sensitivity and specificity, the accuracy of the model prediction was evaluated using the calibration curve, and the clinical application value of the model was evaluated using the decision curve analysis (DCA).Visualising the model by drawing a nomogram.

Some previous studies had reported that the size of lung cancer was closely related to the incidence of LVI [4, 5], and the larger the lesion, the higher the incidence of LVI; however, the larger the lesion, the later the clinical stage and the worse the prognosis of the patient, and the prediction of LVI status of the lesion at this time was not very practical in clinical practice, while prediction of the LVI status of early lung cancer was of great significance for the selection of the surgical and post-operative treatment of lung cancer patients. The size of the lesion was closely related to the clinical staging of lung cancer, and 3 cm had a great role as the watershed between T1 and T2 stages in T staging, and the prognosis of lung cancer ≤ 3 cm was better than that > 3 cm, therefore, the present study constructed the subgroup clinical model during the patients with tumor diameter ≤ 3 cm..

Missing value handling and standardisation of data

This study identified methods for filling in missing values based on data type and used the interpolation fill for the inaccurate data [10]. In order to improve the data quality and ensure the accuracy, consistency and usability of the data, we have standardised the raw medical data collected.

Statistical analysis

Baseline data analysis was performed using SPSS software (Version 22.0, IBM). For continuous variables, the t-test was used if they conformed to normal distribution, and the u-test was used if they did not conform to normal distribution. The continuous variables in our study conformed to normal distribution and were analysed using the T-test, and for categorical variables, the Yates's chi-squared test was used for data analysis. Other statistical analyses were performed using the R package (Version 4.1.0, http://www.Rproject.org). Clinical independent predictors were screened using univariate and multivariate logistic regression analysis. Predictive models were constructed using logistic regression algorithms. Receiver operating characteristic curve (ROC) was used to assess the predictive efficacy of the models for LVI in lung adenocarcinoma. AUC, sensitivity, specificity and accuracy were analysed to assess the efficacy of the model. A cross-validation method was used to calculate the C-index values of the training set and test set to assess the 95% CI of the AUC [11, 12].

Results

Clinical and CT characteristics

The characteristics of the entire study population are summarized in Table 1. LVI-positive and LVI-negative patients accounted for 54.11% ($n=171$) and 45.89% ($n=145$) of the training set, respectively, and for 54.48% ($n=73$) and 45.52% ($n=61$) of the test set, respectively. We assessed the differences between LVI-positive and LVI-negative patients with respect to age, sex, smoking history, carcinoembryonic antigen (CEA) level, tumor diameter, location, border, shape, spiculation, lobulation, vacuole sign, air bronchogram, and pleural indentation in the training and test sets. T-test and chi-square test were used to analyse the data. In the training set, there were significant differences between LVI-positive and LVI-negative patients with respect to CEA level, tumor diameter, spiculation, lobulation, and vacuole sign. In the test set, there were significant differences between

Table 1 Clinical characteristics and CT features of patients in the training and test sets

Characteristics	Training set			Test set		
	LVI-positive ($n=171$)	LVI-negative ($n=145$)	*P* value	LVI-positive ($n=73$)	LVI-negative ($n=61$)	*P* value
Age, years (mean ± SD)	56.90 ± 9.80	58.50 ± 9.70	0.144	57.50 ± 9.60	59.50 ± 9.50	0.227
Sex, n (%)			0.145			0.094
Male	100 (58.50)	72 (49.70)		44 (60.30)	27 (44.30)	
Female	71 (41.50)	73 (50.30)		29 (39.70)	34 (55.70)	
Smoking history, n (%)			0.506			0.776
No	112 (65.50)	101 (69.70)		53 (72.60)	42 (68.90)	
Yes	59 (34.50)	44 (30.30)		20 (27.40)	19 (31.10)	
CEA(ng/mL), n (%)			$P<0.001$			0.030
≤ 5	86 (50.30)	110 (75.90)		45 (61.60)	49 (80.30)	
> 5	85 (49.70)	35 (24.10)		28 (38.40)	12 (19.70)	
Diameter(cm), (mean ± SD)	3.10 ± 1.30	2.00 ± 0.90	$P<0.001$	3.20 ± 1.50	2.20 ± 0.90	$P<0.001$
Location, n (%)			0.384			0.040
Left lung	79 (46.20)	59 (40.70)		21 (28.80)	29 (47.50)	
Right lung	92 (53.80)	86 (59.30)		52 (71.20)	32 (52.50)	
Border, n (%)			1.000			0.506
Sharp	149 (87.10)	127 (87.60)		65 (89.00)	51 (83.60)	
Ill-defined	22 (12.90)	18 (12.40)		8 (11.00)	10 (16.40)	
Shape, n (%)			0.243			0.925
Regular	82 (48.00)	80 (55.20)		39 (53.40)	34 (55.70)	
Irregular	89 (52.00)	65 (44.80)		34 (46.60)	27 (44.30)	
Spiculation, n (%)			$P<0.001$			$P<0.001$
Absent	56 (32.70)	87 (60.00)		20 (27.40)	39 (63.90)	
Present	115 (67.30)	58 (40.00)		53 (72.60)	22 (36.10)	
Lobulation, n (%)			$P<0.001$			$P<0.001$
Absent	43 (25.10)	66 (45.50)		14 (19.20)	31 (50.80)	
Present	128 (74.90)	79 (54.50)		59 (80.80)	30 (49.20)	
Vacuole sign, n (%)			0.025			0.358
Absent	162 (94.70)	126 (86.90)		67 (91.80)	52 (85.20)	
Present	9 (5.30)	19 (13.10)		6 (8.20)	9 (14.80)	
Air bronchogram, n (%)			0.177			0.306
Absent	165 (96.50)	134 (92.40)		71 (97.30)	56 (91.80)	
Present	6 (3.50)	11 (7.60)		2 (2.70)	5 (8.20)	
Pleural indentation, n (%)			0.947			1.000
Absent	82 (48.00)	71 (49.00)		33 (45.20)	28 (45.90)	
Present	89 (52.00)	74 (51.00)		40 (54.80)	33 (54.10)	

Data in parentheses are percentages

LVI Lymphovascular invasion, *SD* Standard deviation, *CEA* Carcinoembryonic antigen

LVI-positive and LVI-negative patients with respect to CEA level, tumor diameter, location, spiculation, and lobulation ($P<0.05$). There was no significant difference with respect to the other characteristics ($P>0.05$) in both sets.

Univariate and multivariate analysis

The results of univariate and multivariate logistic analysis are shown in Table 2. Our characteristics included age, gender, smoking history, CEA level, tumor maximum diameter, tumor location, border, shape, spiculation, lobulation, vacuole sign, air bronchogram and pleural indentation. Univariate and multivariate logistic regression analysis were used to screen independent predictors. We found a significant association of CEA level ($P<0.001$), tumor diameter ($P<0.001$), spiculation ($P<0.001$), lobulation ($P<0.001$), and vacuole sign ($P=0.018$) with LVI. These variables associated with P values <0.05 were further included in the multivariate logistic regression analysis, and the results showed that CEA (OR, 2.060;

Table 2 Results of univariate and multivariate logistic regression analysis showed factors associated with LVI

Characteristics	Univariate analysis		Multivariate analysis	
	OR (95% CI)	*P* value	OR (95% CI)	*P* value
Age, years (mean ± SD)	0.983 (0.961–1.006)	0.145		
Sex, n (%)		0.117		
Male	Reference			
Female	1.428 (0.915–2.230)			
Smoking history, n (%)		0.432		
No	Reference			
Yes	1.209 (0.753–1.943)			
CEA (ng/mL), n (%)		*P* < 0.001		0.009
≤ 5	Reference		Reference	
> 5	3.106 (1.914–5.042)		2.060 (1.200–3.540)	
Diameter, cm (mean ± SD)	2.609 (1.972–3.453)	*P* < 0.001	2.280 (1.700–3.060)	*P* < 0.001
Location, n (%)		0.325		
Left lung	Reference			
Right lung	0.799 (0.511–1.250)			
Border, n (%)		0.904		
Sharp	Reference			
Ill-defined	1.042 (0.535–2.028)			
Shape, n (%)		0.201		
Regular	Reference			
Irregular	1.336 (0.857–2.082)			
Spiculation, n (%)		*P* < 0.001		0.001
Absent	Reference		Reference	
Present	3.080 (1.943–4.884)		2.660 (1.520–4.640)	
Lobulation, n (%)		*P* < 0.001		
Absent	Reference			
Present	2.487 (1.546–4.001)			
Vacuole sign, n (%)		0.018		0.035
Absent	Reference		Reference	
Present	0.368 (0.161–0.842)		0.370 (0.140–0.930)	
Air bronchogram, n (%)		0.118		
Absent	Reference			
Present	0.443 (0.160–1.229)			
Pleural indentation, n (%)		0.858		
Absent	Reference			
Present	1.041 (0.669–1.621)			

LVI Lymphovascular invasion, *OR* Odds ratio, *CI* Confidence interval, *CEA* Carcinoembryonic antigen

95% CI: 1.200–3.540), tumor diameter (OR, 2.280; 95% CI: 1.700–3.060), spiculation (OR, 2.660; 95% CI: 1.520–4.640), and vacuole sign (OR, 0.370; 95% CI: 1.140–0.930) were independent predictors for LVI in LAC.

Construction of the nomogram and evaluation of its diagnostic performance

Based on the final regression analysis, CEA level ($P=0.009$), tumor diameter ($P<0.001$), spiculation ($P=0.001$), and vacuole sign ($P=0.035$) were selected for construction of the nomogram, an example of the clinical application of the nomogram was shown in Fig. 4a. The ROC curves of training and test sets are shown in Fig. 4b. The AUC of the nomogram was 0.800 (95% CI 0.750–0.850) and 0.790 (95% CI 0.710–0.860) in the training and test sets, respectively. The accuracy, sensitivity, and specificity of the nomogram for the training set were 0.741, 0.708, and 0.779, while those for the test set were 0.724, 0.712, and 0.738, respectively (Table 3). The calibration curve showed good calibration of the nomogram in the training and test sets (Fig. 4c, d). The DCA showed that the nomogram had the highest clinical net benefit rate within a threshold range of 0.20–0.85 (Fig. 4e).

Construction of the subgroup model and evaluation of its diagnostic performance

321 patients with diameter ≤ 3 cm were screened from 450 lung cancer patients. Similarly univariate and multivariate logistic regression analysis of clinical factors were performed in all patients. As shown in Table 4, univariate logistic regression analysis showed statistically significant differences in CEA, tumour diameter, spiculation and lobulation sign, and multivariate logistic regression analysis showed that CEA, tumour diameter, and spiculation sign were risk factors for LVI positivity in patients with ≤ 3 cm diameter. The subgroup clinical model

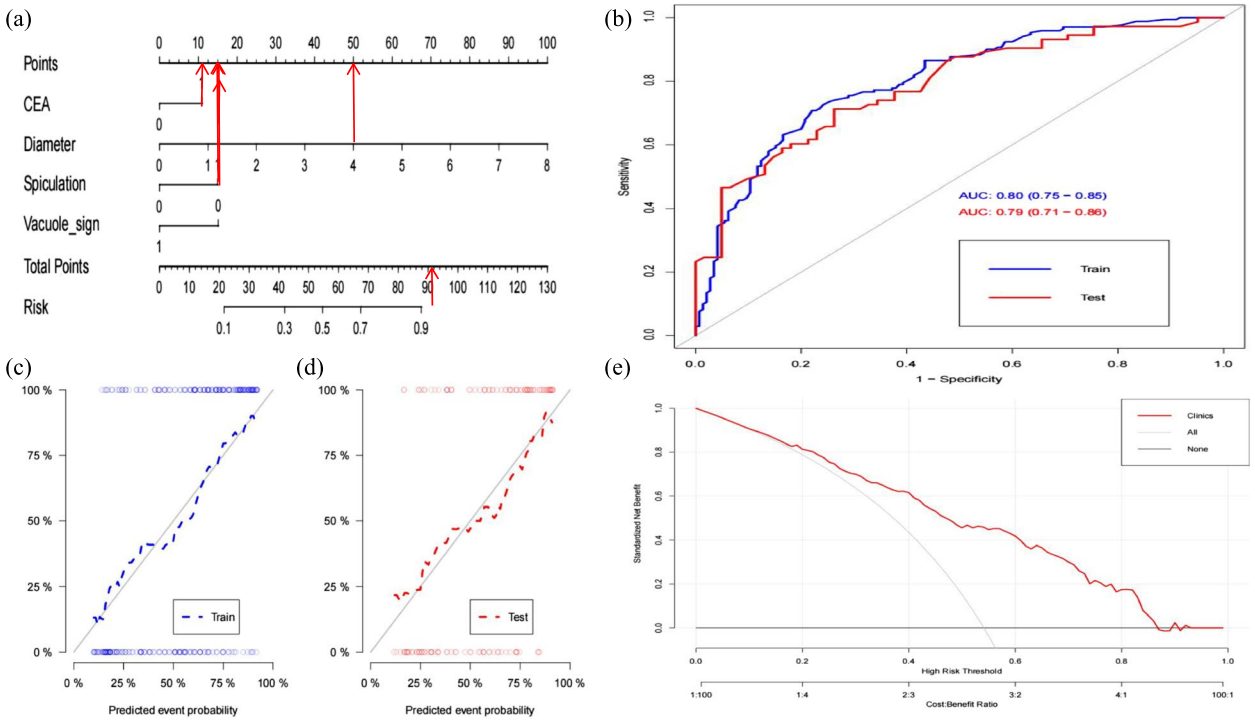

Fig. 4 The nomogram was constructed by combining CEA (0 represents ≤ 5 ng/mL; 1 represents > 5 ng/mL), maximum diameter, spiculation (0 represented absence of the sign; 1 represented presence of the sign), vacuole sign (0 represented absence of the sign; 1 represented presence of the sign). Each variable was awarded a score on the point scale axis. The total score was obtained by adding each single score and by projecting the total score to the lower total point scale, the estimated probability of lymphovascular invasion in lung adenocarcinoma could be obtained, there was an example of the nomogram in clinical application (**a**). The ROC curves of the nomogram (**b**), including training set (AUC = 0.800) and test set (AUC = 0.790). The calibration curves for the nomogram. The x-axis represented the nomogram-predicted probability and the y-axis represented the actual probability of lymphovascular invasion. Perfect prediction performance would correspond to the 45° black solid line. The calibration curve showed a good calibration of the nomogram in the training and test sets (**c**, **d**). Decision curve analysis based on the multi-parameter model nomogram (**e**). The ordinate represented the net benefit rate, and the abscissa was the threshold probability. Red line represented the nomogram. Gray curve represented that all patients were LVI-positive. Black transverse lines represented all patients who were LVI-negative. Compared with all LVI-negative patients (black horizontal line) or all LVI-positive patients (grey curve), the nomogram offered the highest clinical net benefit within a threshold range of 0.20–0.85

Table 3 Diagnostic performance of the nomogram

Groups	AUC(95% CI)	Accuracy	Sensitivity	Specificity
Training set	0.800 (0.750, 0.850)	0.741(0.688,0.788)	0.708(0.659,0.802)	0.779(0.654,0.788)
Test set	0.790 (0.710, 0.860)	0.724(0.640,0.798)	0.712(0.634,0.787)	0.738(0.675,0.802)

AUC Area under curve, *CI* Confidence interval

Table 4 Results of univariate and multivariate logistic regression analysis showed factors associated with LVI in patients with tumors ≤ 3 cm

Characteristics	Univariate analysis		Multivariate analysis	
	OR (95% CI)	*P* value	OR (95% CI)	*P* value
Age, years (mean ± SD)	0.984 (0.957–1.012)	0.268		
Sex, n (%)		0.225		
Male	Reference			
Female	1.389 (0.817–2.363)			
Smoking history, n (%)		0.869		
No	Reference			
Yes	0.954 (0.543–1.675)			
CEA (ng/mL), n (%)		0.001	Reference	0.014
≤ 5	Reference		2.190 (1.180–4.080)	
> 5	2.577 (1.438–4.616)		1.880 (1.120–3.160)	
Diameter, cm (mean ± SD)	2.350 (1.450–3.810)	0.001		0.016
Location, n (%)		0.477		
Left lung	Reference			
Right lung	0.824 (0.484–1.405)			
Border, n (%)		0.894		
Sharp	Reference			
Ill-defined	1.053 (0.495–2.239)			
Shape, n (%)		0.579		
Regular	Reference			
Irregular	1.162 (0.684–1.975)			
Spiculation, n (%)		*P* < 0.001	Reference	*P* < 0.0001
Absent	Reference		3.760 (2.080–6.800)	
Present	4.254 (2.399–7.543)			
Lobulation, n (%)		*P* < 0.001		
Absent	Reference			
Present	3.312 (1.840–5.962)			
Vacuole sign, n (%)		0.179		
Absent	Reference			
Present	0.564 (0.244–1.300)			
Air bronchogram, n (%)		0.155		
Absent	Reference			
Present	0.384 (0.103–1.435)			
Pleural indentation, n (%)		0.426		
Absent	Reference			
Present	1.241 (0.729–2.113)			

LVI Lymphovascular invasion, *OR* Odds ratio, *CI* Confidence interval, *CEA* Carcinoembryonic antigen

constructed by combining all independent predictors showed the reliable predictive efficacy (auc of training set and test were both 0.74). The ROC curves of training and test set were shown in Fig. 5. The accuracy, sensitivity, and specificity of the model for the training set were 0.684, 0.656, and 0.705, while those for the test set were 0.667, 0.610, and 0.709, respectively, as Table 5 showed.

Discussion

In the present study, we used a combination of CT features and clinical indicators for preoperative prediction of the risk of LVI of LAC. The nomogram developed in this study was found to be of value in facilitating treatment decision-making. In our study, CEA level, maximum tumor diameter, spiculation, and vacuole sign were independent predictors of LVI. The AUC of the nomogram constructed based on the above variables was 0.800 in the training set and 0.790 in the test set. The calibration curve and DCA demonstrated the high accuracy and good clinical utility of the model as a non-invasive tool for predicting LVI in LAC. The present study likewise confirmed that clinical models were also of great value in the prediction of LVI in patients with lung adenocarcinoma ≤ 3 cm in diameter. The AUCs of trainning and test sets were both 0.74.

CEA level has been shown to be an independent risk factor for LVI in LAC. CEA is an acid glycoprotein which was first found in colon cancer and fetal intestinal tissue; it has since been identified as a marker of various cancers. More than 70% of NSCLC patients have elevated CEA level, especially those with adenocarcinoma. CEA level has been shown to be a useful diagnostic and prognostic marker of lung cancer [13–16]. It is a convenient and low-cost marker. In recent years, some studies have investigated the relationship between CEA level and LVI in lung cancer. However, none of the studies

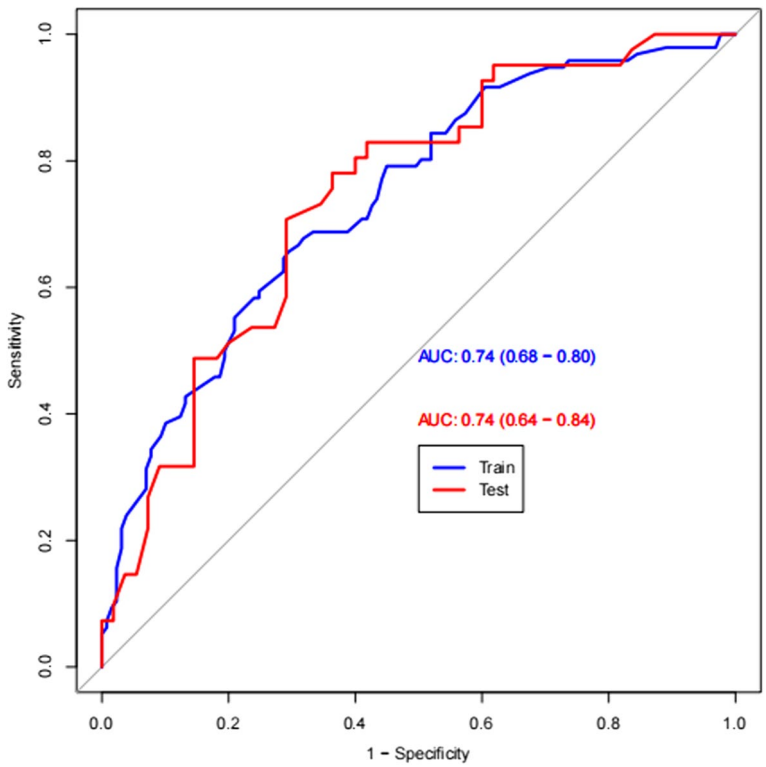

Fig. 5 The ROC curves of the subgroup clinical model in patients with the lesion ≤ 3 cm

Table 5 Diagnostic performance of the clinical model in the subgroup of patients with ≤ 3 cm tumors

Groups	AUC(95% CI)	Accuracy	Sensitivity	Specificity
Training set	0.740 (0.680, 0.800)	0.684(0.619,0.745)	0.656 (0.612,0.756)	0.705 (0.643,0.786)
Test set	0.740 (0.640, 0.840)	0.667(0.563,0.760)	0.610 (0.656,0.789)	0.709 (0.678, 0.785)

AUC Area under curve, *CI* Confidence interval

has characterized the exact relationship between CEA level and LVI in the context of lung cancer. In our study, high preoperative level of CEA was a predictor of LVI in patients with LAC. The higher was the level of CEA, the greater was the probability of LVI. Henderson et al. [17] reported that CEA is a cell adhesion molecule involved in adhesion reactions amongst the cancer cells and between cancer cells and matrix collagen, playing an important role in tumor growth and metastasis. In recent years, a few studies have also found that CEA can interfere with the normal adhesion function of cells, thereby increasing the motility of cancer cells and promoting the dissemination of cancer cells [18]. The above studies explain the molecular basis of the potential correlation between CEA level and the occurrence of LVI. Change in tumor size is an essential indicator of the prognosis and therapeutic efficacy in the context of various tumors. Many studies have also found a close relationship between tumor size and LVI [19–21]. Similarly, Yang et al. [5] identified maximum tumor diameter as an independent risk factor for LVI in LAC ($P=0.027$). In our study, the larger was the tumor diameter, the greater was the probability of LVI. The link between tumor volume and LVI may be explained by the greater requirement of nutrients with increase in the tumor size, leading to increased formation of microvessels, which increases the risk of LVI. Spiculation is one of the common signs of LAC, which is generally attributable to two factors: (1) edema of the interlobular septa around the lesion; (2) infiltration of cancer cells and inflammatory cells in the small blood vessels, lymphatic vessels, and bronchus around the lesion. The pathological basis of the formation of the spiculation varies in benign and malignant lesions. The formation of the spiculation in lung cancer is due to the infiltrative growth and exudative or proliferative reaction of cancer cells. Infiltrative growth of cancer tissue is typically seen along the bronchi, blood vessels, or interlobular septa. Edges often appear as short, thin spiculations. Yang et al. [5] also demonstrated the important value of spiculation in preoperative prediction of LVI in LAC, which was consistent with our study. Interestingly, in our study, LVI-positive patients were relatively less likely to exhibit the vacuole sign. The vacuole sign is manifested as intratumoral low-density shadows sized ≤ 5 mm in diameter on CT, which can be single or multiple, and the upper and lower layers are discontinuous. Previous studies have found that vacuole sign may indicate malignancy, especially in alveolar carcinoma and adenocarcinoma. The pathological basis of the vacuole sign is believed to be the residual gas-containing lung tissue within the tumor or focal bronchiectasis and alveolar space enlargement caused by local bronchial obstruction [22]. The occurrence of vacuole sign is related to the size of the tumor. The larger is the tumor, the lower is the incidence of vacuole sign. Therefore, the vacuole sign is more common in early-stage lung cancer. However, the volume of cancer with LVI is generally larger, which is related to the results of our study. Previous studies have not described the relationship between vacuole sign and LVI in lung cancer; therefore, further studies are required to verify the correlation between the two.

Nomogram is a visual tool used to optimize individualized statistical predictive models, quantify the risk of clinical events based on various risk factors, and provide support for the formulation of treatment plans. Nomograms are widely used in in patients with various tumors [23–25]. A recent study constructed a nomogram to predict LVI in LAC by integrating the maximum diameter of LAC, spiculation, and 2D-Tex-score. The AUC of the training set and the test set were 0.938 and 0.861, respectively. Nie et al. [4] used a combination of LAC components, SUVmax, and CT-radscore to construct a nomogram to predict LVI with good predictive performance. The AUC in the training set and test set were 0.851 and 0.838, respectively [23]. In our study, we investigated clinical factors and CT morphological characteristics that were independent predictors of LVI using univariate and multivariate analysis. Using these factors, we constructed a nomogram, and quantified each variable. The AUC of the established prediction model was 0.790 in the training set and 0.800 in the test set. The nomogram consisted of the predictor variables, different values for each predictor variable correspond to different points, the total points obtained by summing the individual points of all the predictor variables, and the risk value of the disease corresponding to the total points within a certain range. The predictor variables in this study included CEA, tumour diameter, spiculationsign and vacuole sign, each of which corresponded to a different points at different values. In clinical practice, we could assess the exact risk of LVI in each patient based on the points of the specific clinical and CT manifestations of each patient. As shown in Fig. 4a, the patient was a 38 year old male patient and whose LVI status was positive, and the patient's CEA level and spiculation sign were positive, the tumour diameter was 4 cm, and the vacuole sign was negative, the points for the above variables were 10.5, 15, 50, and 15, respectively, and the total points for all variables was 90.5, which was a very intuitive judgement that the risk of this patient for the occurrence of LVI was above 0.9. The clinician could also take further treatment measures based on the risk probability derived from the nomogram, so as to achieve truly individualised treatment. All in all, the nomogram was a statistical model for individualised prediction and analysis

of clinical events, which quantified the risk of clinical events through various risk factors and provided support for the development of treatment plans.

Some limitations of our study should be considered. (1) The model lacked external validation and had a relatively small sample size, which would be further expanded and a multi-centre study would be conducted in the future; (2)Retrospective study could not unified scanning machine, scanning parameters and reconstruction algorithm, and the above factors itself difference would affect the model prediction efficiency, in order to reduce the above impact, our study tried to collect the patients scanning by the same machine, and there were multiple bias in the retrospective study, such as the most common selection bias, often existed the random sampling sample sample could not fully represent the target population, more and more prospective studies were required to verify the accuracy and reliability of the model; (3) We did not include high-dimensional radiomics features parameters, which may help improve the predictive performance of the model.

Conclusion

We developed and validated a novel nomogram for predicting the risk of LVI in patients with LAC in a surgical population. The nomogram is convenient to use and exhibited excellent calibration and clinical utility. The nomogram may help predict the probability of LVI in individual patients, and help improve treatment recommendations for patients with LAC.

Abbreviations

LVI	Lymphovascular invasion
LAC	Lung adenocarcinoma
CT	Computed tomography
CEA	Carcinoembryonic antigen
AUC	Area under the curve
NSCLC	Non-small cell lung cancer
SCLC	Small cell lung cancer
ROC	Receiver operating characteristic
DCA	Decision curve analysis

Clinical trial number

Not applicable.

Authors' contributions

LK designed and supervised the study;LMM,ZX and HHP collected the clinical and CT data of all patients;LMM and LHS analyzed the data;LMM drafted the paper.All authors reviewed the manuscript.

Funding

Guangxi medical and health appropriate technology development and promotion and application project(S20200036).

Data availability

No datasets were generated or analysed during the current study.

Declarations

Ethics approval and consent to participate

The study was approved by the Medical Ethics Commission of the First Affiliated Hospital of Guangxi Medical University and written informed consent was obtained from each participant(Ethical Approval Number: [2023-E153-01]). All the methods included in this study are in accordance with the declaration of Helsinki.

Consent for publication

Not applicable.

Competing interests

The authors declare no competing interests.

Received: 22 November 2023 Accepted: 15 November 2024
Published online: 28 November 2024

References

1. Pathak R, Goldberg SB, Canavan M, Herrin J, Hoag JR, Salazar MC, Papageorge M, Ermer T, Boffa DJ. Association of Survival With Adjuvant Chemotherapy Among Patients With Early-Stage Non-Small Cell Lung Cancer With vs Without High-Risk Clinicopathologic Features. JAMA Oncol. 2020;6(11):1741–50.
2. Bray F, Ferlay J, Soerjomataram I, Siegel RL, Torre LA, Jemal A. Global cancer statistics 2018: GLOBOCAN estimates of incidence and mortality worldwide for 36 cancers in 185 countries. CA Cancer J Clin. 2018;68(6):394–424.
3. Zhang J, Sun J, Liang XL, Lu JL, Luo YF, Liang ZY. Differences between low and high grade fetal adenocarcinoma of the lung: a clinicopathological and molecular study. J Thorac Dis. 2017;9(7):2071–8.
4. Nie P, Yang G, Wang N, Yan L, Miao W, Duan Y, Wang Y, Gong A, Zhao Y, Wu J, et al. Additional value of metabolic parameters to PET/CT-based radiomics nomogram in predicting lymphovascular invasion and outcome in lung adenocarcinoma. Eur J Nucl Med Mol Imaging. 2021;48(1):217–30.
5. Yang G, Nie P, Zhao L, Guo J, Xue W, Yan L, Cui J, Wang Z. 2D and 3D texture analysis to predict lymphovascular invasion in lung adenocarcinoma. Eur J Radiol. 2020;129: 109111.
6. Qin X, Gu X, Lu Y, Zhou W. EGFR-TKI-sensitive mutations in lung carcinomas: are they related to clinical features and CT findings? Cancer Manag Res. 2018;10:4019–27.
7. Cheng Z, Shan F, Yang Y, Shi Y, Zhang Z. CT characteristics of non-small cell lung cancer with epidermal growth factor receptor mutation: a systematic review and meta-analysis. BMC Med Imaging. 2017;17(1):5.
8. Neri S, Menju T, Sowa T, Yutaka Y, Nakajima D, Hamaji M, Ohsumi A, Chen-Yoshikawa TF, Sato T, Sonobe M, et al. Prognostic impact of microscopic vessel invasion and visceral pleural invasion and their correlations with epithelial-mesenchymal transition, cancer stemness, and treatment failure in lung adenocarcinoma. Lung Cancer. 2019;128:13–9.
9. Neri S, Yoshida J, Ishii G, Matsumura Y, Aokage K, Hishida T, Nagai K. Prognostic impact of microscopic vessel invasion and visceral pleural invasion in non-small cell lung cancer: a retrospective analysis of 2657 patients. Ann Surg. 2014;260(2):383–8.
10. Heymans MW, Twisk JWR. Handling missing data in clinical research. J Clin Epidemiol. 2022;151:185–8.
11. LeDell E, Petersen M, van der Laan M. Computationally efficient confidence intervals for cross-validated area under the ROC curve estimates. Electron J Stat. 2015;9(1):1583–607.
12. Droppelmann G, Tello M, García N, Greene C, Jorquera C, Feijoo F. Lateral elbow tendinopathy and artificial intelligence: Binary and multilabel findings detection using machine learning algorithms. Front Med (Lausanne). 2022;9:945698.
13. Dal Bello MG, Filiberti RA, Alama A, Orengo AM, Mussap M, Coco S, Vanni I, Boccardo S, Rijavec E, Genova C, et al. The role of CEA, CYFRA21-1 and NSE in monitoring tumor response to Nivolumab in advanced non-small cell lung cancer (NSCLC) patients. J Transl Med. 2019;17(1):74.

14. de Jong C, Deneer VHM, Kelder JC, Ruven H, Egberts TCG, Herder GJM. Association between serum biomarkers CEA and LDH and response in advanced non-small cell lung cancer patients treated with platinum-based chemotherapy. Thorac Cancer. 2020;11(7):1790–800.
15. Nasralla A, Lee J, Dang J, Turner S. Elevated preoperative CEA is associated with subclinical nodal involvement and worse survival in stage I non-small cell lung cancer: a systematic review and meta-analysis. J Cardiothorac Surg. 2020;15(1):318.
16. Jiao Z, Cao S, Li J, Hu N, Gong Y, Wang L, Jin S. Clinical Associations of Preoperative and Postoperative Serum CEA and Lung Cancer Outcome. Front Mol Biosci. 2021;8:686313.
17. Henderson RA, Finn OJ. Human tumor antigens are ready to fly. Adv Immunol. 1996;62:217–56.
18. Huang JY, Zhao L, Lei W, Wen W, Wang YJ, Bao T, Xiong HY, Zhang XH, Wang SF. A high-sensitivity electrochemical aptasensor of carcinoembryonic antigen based on graphene quantum dots-ionic liquid-nafion nanomatrix and DNAzyme-assisted signal amplification strategy. Biosens Bioelectron. 2018;99:28–33.
19. Lin S, Ye F, Rong W, Song Y, Wu F, Liu Y, Zheng Y, Siqin T, Zhang K, Wang L, et al. Nomogram to Assist in Surgical Plan for Hepatocellular Carcinoma: a Prediction Model for Microvascular Invasion. J Gastrointest Surg. 2019;23(12):2372–82.
20. Ouyang FS, Guo BL, Huang XY, Ouyang LZ, Zhou CR, Zhang R, Wu ML, Yang ZS, Wu SK, Guo TD, et al. A nomogram for individual prediction of vascular invasion in primary breast cancer. Eur J Radiol. 2019;110:30–8.
21. Oliver-Perez MR, Magriña J, Villalain-Gonzalez C, Jimenez-Lopez JS, Lopez-Gonzalez G, Barcena C, Martinez-Biosques C, Gil-Ibañez B, Tejerizo-Garcia A. Lymphovascular space invasion in endometrial carcinoma: Tumor size and location matter. Surg Oncol. 2021;37:101541.
22. Xiang W, Xing Y, Jiang S, Chen G, Mao H, Labh K, Jia X, Sun X. Morphological factors differentiating between early lung adenocarcinomas appearing as pure ground-glass nodules measuring ≤10 mm on thin-section computed tomography. Cancer Imaging. 2014;14(1):33.
23. Hu HT, Wang Z, Huang XW, Chen SL, Zheng X, Ruan SM, Xie XY, Lu MD, Yu J, Tian J, et al. Ultrasound-based radiomics score: a potential biomarker for the prediction of microvascular invasion in hepatocellular carcinoma. Eur Radiol. 2019;29(6):2890–901.
24. Jin C, Cao J, Cai Y, Wang L, Liu K, Shen W, Hu J. A nomogram for predicting the risk of invasive pulmonary adenocarcinoma for patients with solitary peripheral subsolid nodules. J Thorac Cardiovasc Surg. 2017;153(2):462-469.e461.
25. Shao C, Feng X, Yu J, Meng Y, Liu F, Zhang H, Fang X, Li J, Wang L, Jiang H, et al. A nomogram for predicting pancreatic mucinous cystic neoplasm and serous cystic neoplasm. Abdom Radiol (NY). 2021;46(8):3963–73.

Publisher's Note